Timing and Precision of Spike Initiation in Layer V Pyramidal Cells of the Rat Somatosensory Cortex

Thomas Berger and Hans-R. Lüscher

Institute of Physiology, University of Bern, Bühlplatz 5, CH 3012 Bern, Switzerland

The timing and location of action potential initiation in layer V pyramidal cells of the rat somatosensory cortex depends on different ligand-gated and intrinsic conductances. In order to assess the shunting effect of $GABA_A$ receptor activation and I_h on the summative properties of these neurons, we recorded simultaneously from their somata and dendrites and induced combined excitatory and inhibitory postsynaptic potentials using extracellular stimulation. Three major consequences of $GABA_A$ receptor activation on the integration properties were found: (i) the action potential could be initiated in the distal apical dendrite, if $GABA_A$ receptors were simultaneously activated in the soma; (ii) $GABA_A$ receptor activation narrowed the time window for suprathreshold summation of two coincident excitatory synaptic inputs by a factor of 3.4; and (iii) uneven weights of the GABAergic components between two inputs could lead to unbalanced shunting and consequently to a time shift in the peak of the coincidence detection window. Blockade of I_h practically abolished coincidence detection within a time window of 30 ms. Location of spike initiation and summation of coincident inputs in pyramidal cells is determined by at least two shunting mechanisms: activation of the presynaptic inhibitory network and modulation of I_h as a function of the postsynaptic membrane potential.

Introduction

The layer V pyramidal cell of the somatosensory cortex operates with two spike initiation zones. A low-threshold sodium spike is initiated in the initial segment of the axon, whereas a high-threshold calcium spike may be generated in the distal apical dendrite (Schiller *et al*., 1997). Different conductances and the localization of the inputs influence the synaptic integration and firing pattern as well as the origin of spike generation (Larkum *et al*., 1999, 2001; Williams and Stuart, 2002). In principal, neurons can operate in two distinct ways, depending on the duration of the interval over which they effectively summate incoming synaptic potentials. If this interval is of the order of the mean interspike interval or longer, neurons act effectively as temporal integrators and transmit temporal patterns with only low reliability. If, by contrast, the integration interval is short compared to the interspike interval, neurons act essentially as coincidence detectors and the temporal structure of their output is a direct function of the input pattern. Cortical neurons and dendrites with active conductances are able to act as coincidence detectors (König *et al*., 1996; deCharms and Zador, 2000; Pouille and Scanziani, 2001). However, there is an ongoing discussion about the importance of coincidence detection versus temporal integration for information processing in cortical areas (Gray, 1999; Shadlen and Movshon, 1999) and theoretical work has shown that passive-membrane model neurons can act as both coincidence detectors and temporal integrators (Kisley and Gerstein, 1999). The precision of coincidence detection should depend on mechanisms which curtail excitatory postsynaptic potentials (EPSPs) and thereby limit summative processes – such as GABAergic inhibition (Funabiki *et al*., 1998; Pouille and Scanziani, 2001) or the hyperpolarization-activated current, I_h (Berger *et al*., 2001). The GABAergic interneurons of the cortex set up distinct networks coupled via GABAA receptors and gap junctions (Gibson *et al*., 1999). The soma of pyramidal cells is nearly exclusively covered with symmetric, putative GABAergic synapses, while asymmetric, putative glutamatergic synapses are found on the dendritic spines (White, 1989; Farinas and DeFelipe, 1991). Activation of these networks should have a strong impact on the integrative functions of layer V pyramidal cells. In addition, an I_h conductance (Pape, 1996) is present in high density along the apical dendrites of layer V pyramidal cells (Santoro *et al*., 1997; Williams and Stuart, 2000; Berger *et al*., 2001). The density of I_h increases nonlinearly with distance from the soma and reaches very high values in the distal apical dendrite (Berger *et al*., 2001).

In order to study the impact of $GABA_A$ receptors and I_h on synaptic integration and coincidence detection, we activated synaptic inputs in layer V pyramidal cells using extracellular stimulation. This induced a barrage of excitatory and inhibitory events, which were spatially distributed over the entire neuron. Such a heterogeneous situation may actually reflect the physiological input of a pyramidal cell at a given time. This experimental approach enabled us to assess true conductance changes in contrast to direct current injection into a neuron. Under these conditions, activation of $GABA_A$ receptors and deactivation of I_h influenced the localization of spike generation and defined the width and symmetry of the time window for coincidence detection.

Materials and Methods

Brain Slice Preparation and Cell Identification

Parasagittal slices (300 μm thick) of the somatosensory cortex were prepared from 28–35-day-old Wistar rats according to national and institutional guidelines. Preparations were carried out in ice-cold extracellular solution using a vibratome (752M, Campden Instruments, Loughborough, UK, or Microslicer DTK-1000, Dosaka, Kyoto, Japan). Slices were incubated at 37°C for 30–60 min and then left at room temperature until recording. Layer V pyramidal neurons from the somatosensory area with a thick apical dendrite were visualized by infrared differential interference contrast videomicroscopy utilizing a Newvicon camera (C2400; Hamamatsu, Hamamatsu City, Japan) and an infrared filter (RG9; Schott, Mainz, Germany) mounted on an upright microscope (Axioskop FS Zeiss, Oberkochen, Germany).

Recordings

Current-clamp whole-cell recordings were either made from the soma alone or simultaneously from the soma and apical dendrite of layer V pyramidal neurons. Simultaneous somatic and dendritic recordings were made to estimate the location of the activated synapses and to study the origin of action potentials. An Axoprobe-1A amplifier (Axon Instruments, Foster City, CA) was used. Resistance compensation and capacitance

neutralization were applied. Electrodes were made from borosilicate glass tubing with or without 20% PbO (Hilgenberg, Malsfeld, Germany). The resistance was 3–5 MΩ for somatic and 6–11 MΩ for dendritic recording pipettes. All experiments were carried out at ~34°C. Data were low-pass filtered at 5 kHz using the internal filter of the amplifier. The sampling frequency was twice the filter frequency. Data were digitized and stored on-line using Clampex8 (Axon Instruments) connected to a personal computer. Data were analyzed off-line with Clampfit8. Pooled data are expressed as mean ± standard deviation (SD) and statistical significance was assessed by one-way analysis of variance (ANOVA) with significance levels of 0.05 or 0.01.

Stimulation

Bipolar stimulation electrodes were made from twisted pairs of insulated nickel–chromium wire (diameter 25 μm; Goodfellow, Cambridge, UK). Two of these stimulation electrodes were glued into one pipette and their distance was adjusted to ~600 μm. Prior to recording, their tips were placed on the surface of the slice at the border between layers I and II in such a way that the apical dendrite had a horizontal distance of ~300 μm from each of the electrodes. Because we did not cut the slice from white matter to layer II/III (Cauller and Connors, 1994; Zhu, 2000), synaptic inputs were likely activated in all layers along the somatodendritic axis of the cell under study (Yuste *et al.*, 1994). Consequently, the PSP elicited by one stimulation electrode consisted of excitatory and inhibitory inputs from different regions of the cell. In order to make the coincidence detection window under control and blocking conditions comparable, we adjusted the stimulation intensity in such a way that the spiking probability in the postsynaptic neuron was ~50% with simultaneous stimulation of the two sites (threshold criterion; see Fig. 6) (Pouille and Scanziani, 2001).

Chemicals and Solutions

Slices were continuously superfused with a physiological extracellular solution (containing, in mM: NaCl, 125; $NaHCO_3$, 25; KCl, 2.5; NaH_2PO_4, 1.25; $CaCl_2$, 2; $MgCl_2$, 1; glucose, 20), bubbled with 95% O_2 and 5% CO_2. The pipette solution contained (in mM): K-gluconate, 110; KCl, 30; EGTA, 10; HEPES, 10; Mg-ATP, 4; Na_2-GTP, 0.3; Na_2-phosphocreatine, 10; the solution was pH adjusted to 7.3 with KOH.

ZD7288 [4-(*N*-ethyl-*N*-phenylamino)-1,2-dimethyl-6-(methylamino) pyridinium chloride] was a generous gift of Astra-Zeneca (Macclesfield, UK). CNQX [6-cyano-7-nitroquinoxaline-2,3-dione] and gabazine [6-imino-3-(4-methoxyphenyl)-1(6H)-pyridazinebutanoic acid hydrobromide] were bought from Tocris Cookson (Bristol, UK). All other drugs and chemicals were from Sigma or Merck. Stock solutions of 50 mM ZD7288, 10 mM bicuculline methiodide and 3 mM gabazine were prepared in bidistilled water; a stock solution of 10 mM CNQX was made in dimethylsulfoxide. Dilution in the extracellular solution provided the final concentrations given in the Results section.

Results

The results are structured as follows. First, simultaneous somatic and dendritic recordings were used to identify the predominant site of synaptic inputs. Secondly, the independence of the activated inputs was tested. Thirdly, the effect of $GABA_A$ receptor activation on the origin of the action potential was determined. Fourthly, the effect of $GABA_A$ receptor activation and I_h deactivation on the symmetry and width of the coincidence detection time window is presented.

Localization of the Input and Spike Initiation Zone

We activated synaptic inputs with extracellular stimulation electrodes situated at the border between layers I and II — one on either side of the cell (Fig. 1*A*). The composite postsynaptic potentials (PSPs) induced by one stimulation electrode had a mean amplitude of 11.8 ± 3.7 mV (n = 116 inputs) at the soma (membrane potential at the soma = –68.4 ± 6.4 mV, n = 58 cells). In simultaneous somatic and dendritic recordings (range of the interelectrode distances 200–430 μm, mean distance ± SD = 320 ± 76 μm, n = 17 cells), we could identify the approximate origin of the majority of the activated synaptic inputs (Berger *et al.*, 2001). For PSPs originating distally or close to the dendritic electrode (e.g. in the tuft), the amplitude attenuated, while time to peak and latency of the PSPs increased from the distal to the somatic recording site (Fig. *1B*). PSPs generated primarily at the basal dendrites and the soma showed the opposite behavior (Fig. 1*C*). Activation of all 17 proximally located inputs with a suprathreshold stimulation intensity induced a somatic spike and a resulting back-propagating dendritic action potential (Fig. 1*E*). In contrast, in eight out of seventeen distally located inputs, suprathreshold stimulation intensity induced a dendritic, forward-propagated sodium-calcium action potential (Larkum *et al.*, 2001), which was followed by a somatic sodium spike (Fig. 1*D*). However, activation of the other nine distally located inputs resulted in a somatic action potential, which back-propagated into the dendrite (not shown).

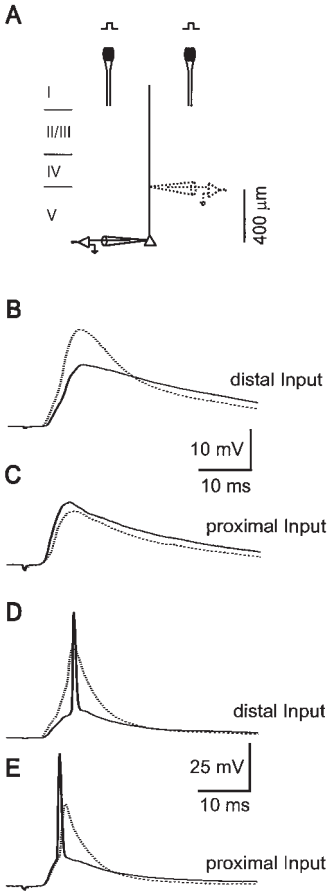

Figure 1. The impact of synaptic localization on spike generation. (*A*) Position of the two recording electrodes at the soma and the apical dendrite and the two bipolar stimulation electrodes on either side of a layer V pyramidal cell. (*B–E*) Recordings from the same cell, dendritic recording 400 μm from the soma. Somatic membrane potential (V_m) = –73 mV. Somatic recordings, solid traces; dendritic recordings, dotted traces. (*B*, *C*) Subthreshold stimulation of one input activated primarily distally located synapses (*B*), that of the other input activated primarily proximally located synapses (*C*) in this cell. (*D*, *E*) Suprathreshold activation of the distal input induced in this cell dendritic sodium–calcium spikes forward-propagating to the axonal spike initiation zone (*D*), while suprathreshold activation of the proximal input induced somatic spikes which were back-propagating into the dendrite (*E*).

Independence of Combined Inputs

The stimulation strength (40–300 μA, 100–500 μs) was adjusted

in such a way that the activation of a single stimulation electrode ('input') did not evoke an action potential, while the simultaneous activation of both stimulation electrodes elicited a spike with a probability of ~50%. The stimulation intensity had to be adjusted under certain blocking conditions (see below) to match this threshold criterion. To exclude the possibility that the activation of one input led to the presynaptic refractoriness of the other input, a slope ratio was calculated – see Fig. 2*A*,*B* (Pouille and Scanziani, 2001). The slope ($\Delta V/\Delta t$) of the averaged PSP was determined during the first millisecond of the rise after the onset of the PSP. The two inputs were considered to be independent, i.e. two different sets of synapses were activated, if the slope of the PSP after simultaneous activation resulted in a value of at least 80% of the arithmetic sum of the slopes of the two individual inputs (Fig. 2*A*). In 13 out of 58 cells studied a lower slope ratio was found, suggesting that the two inputs were partially overlapping (Fig. 2*B*). Only the data from independent inputs were used.

In order to study the mechanisms underlying synaptic integration and coincidence detection of two inputs to layer V pyramidal cells, one input was always activated at the same relative time while the second input was activated between 30 ms before and 30 ms after this first input, with 5 ms increments (Fig. 2*C*,*D*). The interval between the combined activation of the inputs was 5 s to prevent paired pulse facilitation or depression. In order to calculate a spiking probability in the postsynaptic neuron after activation of two inputs with a defined delay, the protocol with different delays was repeated between 10 and 40 times ('runs'). The number of spikes was counted for each delay and divided by the number of runs, thus yielding the probability for a spike at a given inter-stimulus delay (mean spiking probability, MSP; Fig. 2*E*,*F*). If pharmacological tools changed the spiking pattern (bursts versus single spikes), spikes and bursts were considered as equivalent for the calculation of the MSP. With independent inputs, the probability was highest with zero or a small delay between the two inputs (Fig. 2*C*), resulting in a plot of the MSP versus input delay with a singular peak (Fig. 2*E*). With partially overlapping inputs, spikes were not induced if the PSPs were highly coincident. This could be due to the fact that both electrodes were stimulating identical axons, which became refractory once activated. However, spikes were evoked if both inputs were sufficiently separated in time, resulting in a plot with two separate peaks (Fig. 2*D*,*F*). This distinct M-shape of the coincidence window was used as an additional criterion for detecting and rejecting data from partially overlapping inputs.

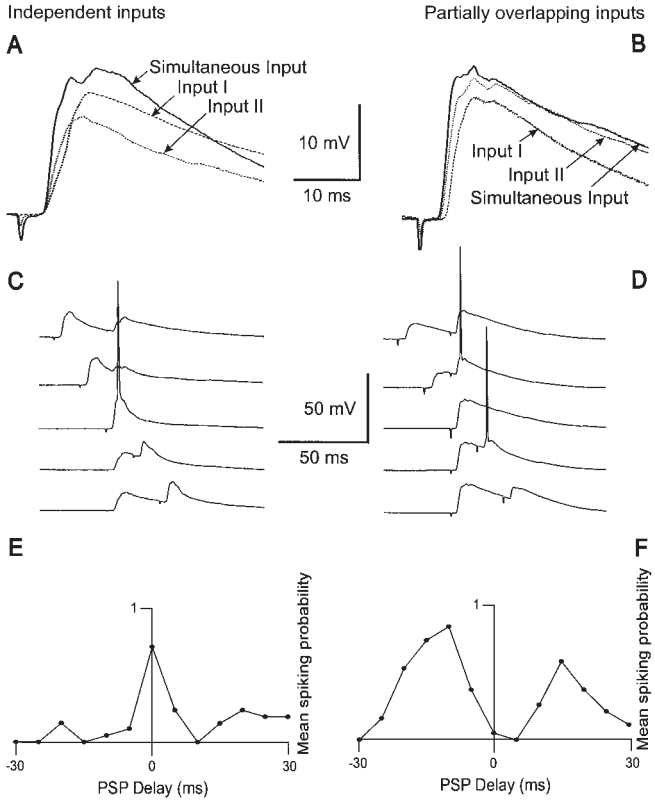

Figure 2. Temporal interactions of independent and partially overlapping inputs. (*A*, *C*, *E*) Independent inputs. (*B*, *D*, *F*) Partially overlapping inputs in another cell. (*A*) With independent inputs, the slope of the rise after simultaneous activation of both inputs (solid trace) was similar to the sum of the rising-phase slopes of the individually activated inputs (dotted traces). (*B*) In contrast, the slope of the rise after combined activation of both inputs (solid trace) was smaller than the sum of the rising-phase slopes of the individually activated inputs (dotted traces) in partially overlapping inputs. (*C*, *D*) Combined activation of both inputs (relative delay –30, –15, 0, 15 and 30 ms). With independent inputs, an action potential was generated when the delay was minimal. If the inputs were partially overlapping, action potentials were only generated with delays of –15 and 15 ms. (*E*, *F*) The mean number of action potentials for each of the thirteen delays (from –30 to 30 ms, with 5 ms increments; total number of spikes for each increment divided by the number of runs). In the case of independent inputs, the highest probability for a spike was at zero delay. If the inputs were partially overlapping, the spike probability had two peaks on either side of 0 ms. In these layer V pyramidal cells, coincident inputs were mutually refractory due to partially overlapping inputs. $V_m = -65$ mV at (*A*, *C*) and $V_m = -70$ mV at (*B*, *D*).

$GABA_A$ Receptors and Spike Initiation

In eight cells it was impossible to induce spikes even with very high stimulation intensities (500–1000 μA, 500 μs). When these cells were depolarized with constant DC current injection, the PSP induced by both stimulation electrodes reversed its sign at –49 ± 6 mV, i.e. close to the Nernst potential for Cl^- (E_{Cl^-} –40 mV with the solutions used). After the application of 10 μM bicuculline, the reversal potential of the PSP shifted to ~0 mV (n = 2 out of 2 tested), the reversal potential of ionotropic glutamate receptors. This suggests that in these cells a prominent $GABA_A$ conductance shortened the decaying phase of the EPSP (cf. Fig. 3*A*,*B*) and thus prevented the generation of action potentials.

The effect of $GABA_A$ receptor activation on synaptic integration or coincidence detection was studied by application of 1 or 10 μM bicuculline to the bath. In additional experiments, 3 μM gabazine (Ito *et al.*, 1992) was used instead of 10 μM bicuculline, resulting in effects which were not distinct from those described below (n = 3; not shown). During $GABA_A$ receptor blockade, we always added 1 μM CNQX to the extracellular solution to prevent epileptic activity in the slice. The stimulation strength had to be changed to 117 ± 25% (n = 12 inputs) and 54 ± 20% (n = 16 inputs) of control for 1 and 10 μM bicuculline, respectively, in order to match the threshold criterion defined above. Overall, the decay time constant of the PSPs was not changed significantly in comparison to the control PSP group, neither in 1 nor in 10 μM bicuculline. However, in some individual experiments an increase in the decay time constant could be seen (Fig. 3*A*,*B*). This heterogeneity in the effect of $GABA_A$ receptor blockade may be due to a heterogeneous contribution of $GABA_A$ receptors to the control PSP (decay time constant under control conditions varied in the range 7.1–76.9 ms, n = 116 inputs). In addition, in some recordings under bicuculline the I_h-induced undershoots (Berger *et al.*, 2001) became more pronounced and shortened the decay kinetics (not shown).

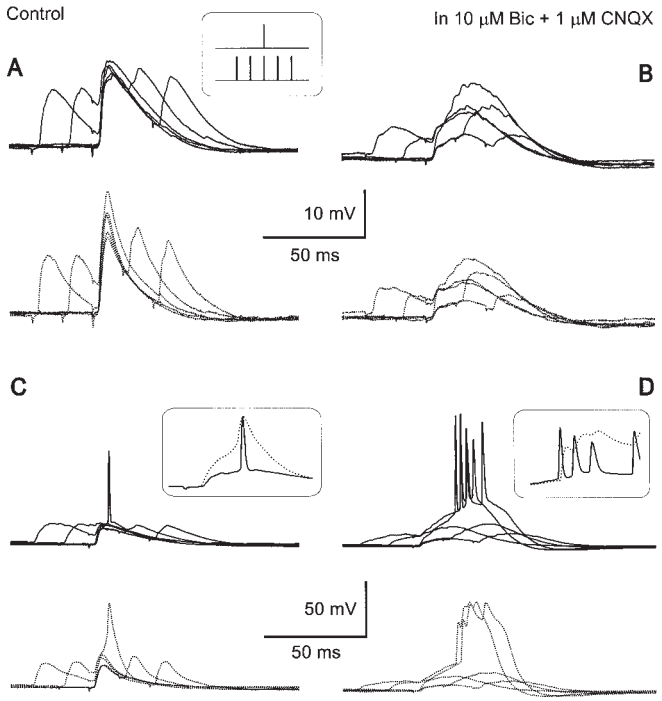

Figure 3. The effect of $GABA_A$ receptors on integration of synaptic events. (*A–D*) Recordings from the same cell, dendritic recording 310 μm from the soma; V_m = –65 mV. Somatic recordings, solid traces; dendritic recordings, dotted traces. (*A*, *B*) Subthreshold recordings. (*C*, *D*) Suprathreshold recordings. (*A*) Under control conditions, two inputs were activated with delays between –30 and 30 ms and an increment of 15 ms (see inset). While the combined synaptic responses summated in the dendrite, this was not the case in the soma. (*B*) With 10 μM bicuculline and 1 μM CNQX, the stimulation intensity had to be reduced to prevent spike generation due to a single input; 1 μM CNQX was added to prevent epileptic events in the slice. Now summation could be seen at both recording locations. The rising phase of the postsynaptic events was multiphasic, suggesting presynaptic bursting activity or polysynaptic excitation. The decaying phase was prolonged. (*C*) A spike was induced when delays between both inputs were minimal. This axonal spike was only activated after a forward-propagating dendritic sodium–calcium spike activated the axonal action potential initiation zone (see inset). (*D*) With 10 μM bicuculline and 1 μM CNQX, somatic bursts and a subsequent combined calcium–sodium spike in the dendrite were induced. The axonal spikes were back-propagating into the dendrite (see inset). These bursts could be induced over a broader time frame in comparison to control, indicating impaired coincidence detection.

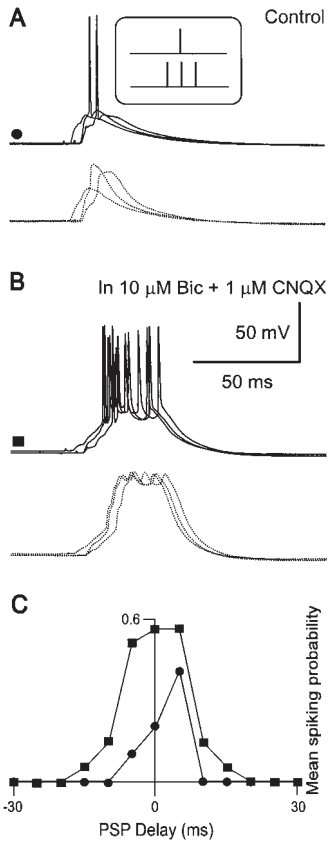

Figure 4. The effect of $GABA_A$ receptors on coincidence detection of synaptic events. (*A*,*B*) Recordings from the same cell, dendritic recording 320 μm from the soma; V_m = –72 mV. Two inputs were activated with delays between –5 and 5 ms and an increment of 5 ms (see inset). Somatic recordings, solid traces; dendritic recordings, dotted traces. (*A*) Under control conditions, the 'variable' input shunted the 'stationary' input but not vice versa. A spike was therefore primarily induced if the variable input had passed the stationary input. (*B*) With 10 μM bicuculline and 1 μM CNQX, the cell started to generate bursts. The time window for coincidence detection was now broadened and became symmetrical to the origin. (*C*) Plot of the PSP delay against the mean spiking probability. Under control conditions (circles), an asymmetrical plot is seen, while under bicuculline (rectangles) the plot became symmetrical, the time window for coincidence detection was widened markedly and the probability for spike generation increased.

$GABA_A$ receptor blockade by bicuculline or gabazine (with 1 μM CNQX) could switch the origin of spike generation and reverse the direction of propagation by enabling somatic PSP summation. In five somatodendritic recordings, summation of the PSPs from both inputs was much less pronounced in the soma than in the dendrite (Fig. 3*A*). In these cases, somatic sodium action potentials were only induced when a local dendritic sodium–calcium spike (Larkum *et al.*, 2001) brought the soma suprathreshold ('forward-propagated action potential'; Fig. 3*C*, inset). The lack of somatic summation and its inability to produce spikes could be abolished by the application of 10 μM bicuculline (Fig. 3*B*,*D*). Under these conditions, the dendritic sodium–calcium spike was seen after the beginning of the somatic burst ('back-propagating action potential'; Fig. 3*D*, inset). The presence of a strong GABAergic input located mainly on the soma was most likely responsible for this observation.

In the majority of the cells, 1 μM bicuculline (n = 5 out of 6) or 10 μM bicuculline (n = 9 out of 9) changed the spiking behavior from single spikes to bursts (Figs 3*C*,*D* and 4*A*,*B*). In addition, the subthreshold PSP showed a multiphasic rise under bicuculline, which could be due to presynaptic burst activity or polysynaptic inputs (Fig. 3*B*). The number of spikes per burst and the delay between both inputs was negatively correlated. However, epileptic activity or spontaneous bursts were not seen. The integral below the MSP–delay curve was taken as a measure of the overall spiking probability and thus of the general excitation due to the activation of the cell's inputs. The overall spiking probability was increased to 257 ± 103% (n = 4) and 488 ± 202% (n = 9) of control for 1 or 10 μM bicuculline, respectively.

$GABA_A$ Receptors and Coincidence Detection

In order to investigate the importance of $GABA_A$ receptor activation for coincidence detection, both inputs were activated as described above. The time window for the generation of spikes and bursts became broader under 1 μM bicuculline (n = 2 cells; not shown), while in two cells no effect was seen. Under 10 μM bicuculline, the time window was always broadened (n = 9 out of 9 cells; Figs 3*C*,*D* and 4). The MSP–delay plots were fitted with a Gaussian function and the SD of this fitted curve increased from 2.8 (n = 13) to 7.6 (n = 4) and 9.5 ms (n = 9) for 1

or 10 μM bicuculline, respectively ($P < 0.05$ using the *F*-distribution test; Fig. 6*A*,*B*). Thus, block of the GABAergic input impaired coincidence detection in the cells under study.

The MSP reflects the probability of eliciting an action potential in a given cell excited by two groups of composite inputs of unknown excitatory and inhibitory contribution. It was not necessarily the case that the MSP was highest when both inputs were activated simultaneously (Fig. 4*A*). In about half of the cells tested ($n = 26$ out of 45 cells), an uneven summation of both inputs was found, resulting in an asymmetric MSP–delay plot (Fig. 4*C*). The mean delay for the peak of the MSP was 9.4 ± 5.1 ms (range 2.5–22.5 ms) in these 26 cells. A shift of the plot from an asymmetric situation to a symmetric one was seen in all cells under 10 μM bicuculline or 3 μM gabazine ($n = 5$ out of 5 cells; Fig. 4*B*,*C*). In order to compare the coincidence detection window of an asymmetric MSP plot under control conditions and the corresponding symmetric MSP plot after blockade of the GABAergic input, we aligned both plots along the time axis. Therefore, their maximal MSP was set to a delay of 0 ms. An asymmetric plot reflects most likely an uneven activation of GABAergic interneurons by the different stimulation electrodes and therefore a different ability of the two inputs to shunt each other.

I_h and Coincidence Detection

In order to study the effect of the hyperpolarization-activated cationic current I_h on coincidence detection, 10 or 100 μM of the specific blocker ZD7288 (Harris and Constanti, 1995) was added to the bath solution. Separate activation of both inputs was carried out under control conditions and in the presence of ZD7288 (Fig. 5*A*,*B*). With 10 μM ZD7288, the stimulation strength was always left unchanged ($n = 8$ inputs). In contrast, with 100 μM ZD7288, the stimulation strength was changed to 93 ± 19% ($n = 28$ inputs) of the control value to match the threshold criterion. The hyperpolarization of ~10 mV induced by ZD7288 (Berger *et al.*, 2001) was always compensated by DC current injection. The monoexponentially fitted mean PSP decay time constant increased to 67.1 ± 23.2 and 81.5 ± 34.2 ms for 10 or 100 μM ZD7288 in comparison to a control value of 32.2 ± 13.9 ms ($P < 0.01$; $n = 8$ inputs and $n = 28$ inputs, respectively; Fig. 5*B*).

The effect of I_h on coincidence detection was studied with the protocols described above. The overall spiking probability increased to 238 ± 81% ($n = 3$ cells) and 401 ± 184% ($n = 12$ cells) of control for 10 or 100 μM ZD7288, respectively. The time window for the generation of spikes was markedly broadened in 100 μM ZD7288 ($n = 12$ cells out of 12; Fig. 5*C*,*D*), while the effect of 10 μM ZD7288 was not statistically significant ($n = 3$ out of 3 cells; not shown). The resulting MSP–delay plot became very broad and independent of the inter-stimulus delay in 100 μM ZD7288 (Fig. 6*C*). With blocked I_h, coincidence detection is therefore practically abolished within the time window tested. In contrast to bicuculline or gabazine, ZD7288 did not change the spiking pattern of the cells, nor did it shift the MSP–delay plot.

In one out of three cells with forward-propagated dendritic spikes, application of 100 μM ZD7288 reversed the propagation direction (Fig. 5*D*, lower four traces). In contrast, in two other cells, 100 μM ZD7288 did not induce a change from forward- to back-propagating spikes (not shown).

The results show that coincidence detection in layer V pyramidal cells of the somatosensory cortex is influenced by at least two conductances. $GABA_A$ receptors as well as I_h sharpen the time window for coincidence detection by curtailing the decaying phase of the PSP. In addition, an unbalanced activation of GABAergic neuron populations can shift the time window for coincidence detection. Bicuculline or ZD7288 can switch the action potential initiation zone from dendrite to soma, with a concomitant reversal in the direction of spike propagation in the apical dendrite.

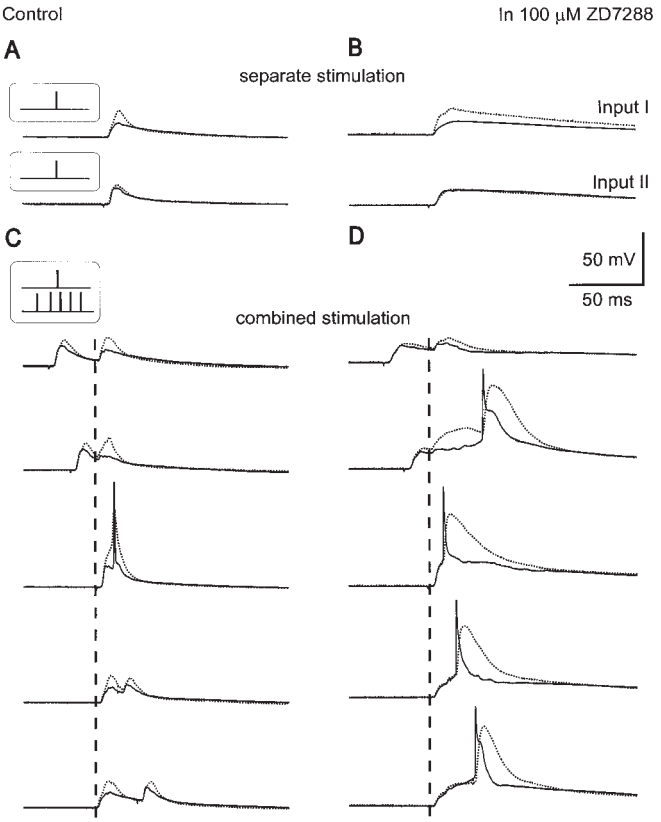

Figure 5. Deactivation of I_h narrows the time window for coincidence detection by shortening the decay phase of the PSPs. (*A–D*) Recordings from the same cell, dendritic recording 400 μm from the soma; same cell as in Fig. 1; $V_m = -73$ mV. Somatic recordings, solid traces; dendritic recordings, dotted traces. (*A*, *B*) Separate stimulation of both inputs (see insets). (*A*) Control conditions. (*B*) When I_h was blocked with 100 μM ZD7288, the decaying phase of the PSPs was strongly prolonged. (*C*,*D*) Variable input was activated with delays between –30 and 30 ms and an increment of 15 ms relative to the stationary input (see inset). (*C*) A forward-propagating dendritic spike leading to an axonal spike was induced only when the inputs were coincident. The traces are aligned to the stimulus artifact of the stationary input (dashed lines). (*D*) With 100 μM ZD7288, the probability for an action potential was independent of the delay between both inputs. The axonal action potential was now back-propagating and the dendritic spikes were markedly prolonged, presumably due to the presence of calcium currents. These, on the other hand, resulted in a more pronounced shoulder of the axonal action potential.

Discussion

The layer V pyramidal cell of the somatosensory cortex is a neuron with inhomogeneous distributions of different voltage- and ligand-gated conductances and two interacting spike initiation zones in the axon and the dendritic tuft linked by the apical dendrite (Magee, 1999; Larkum *et al.*, 2001; Larkum and Zhu, 2002; Migliore and Shepherd, 2002). Synaptic integration along the somatodendritic axis depends on several biophysical factors. We have shown that two of them, namely $GABA_A$ receptors and I_h, have a strong impact on the time window for coincidence detection.

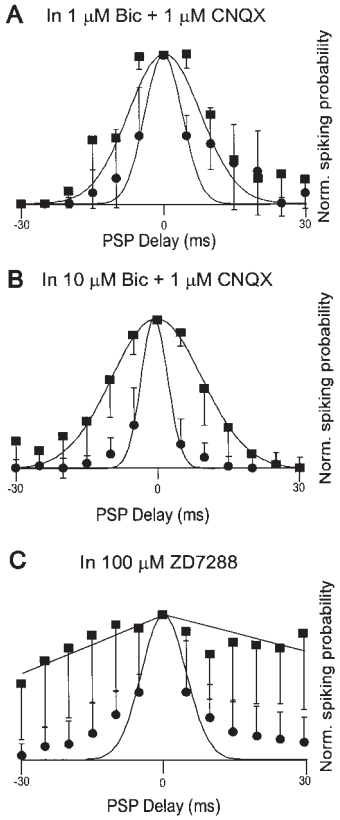

Figure 6. Impact of $GABA_A$ receptors and I_h on coincidence detection. The PSP delay was plotted against the normalized spiking probability under control conditions (circles) and with different blockers (rectangles). The plots were normalized for each cell to the MSP at a delay of 0 ms. (*A*) 1 μM bicuculline and 1 μM CNQX ($n = 4$ cells); curves within the plot are Gaussian fits of the data. (*B*) 10 μM bicuculline and 1 μM CNQX ($n = 9$ cells); curves within the plot are Gaussian fits of the data. (*C*) 100 μM ZD7288 ($n = 12$ cells); curve within the control plot is a Gaussian fit of the data. The data under ZD7288 were fitted with straight lines. While bicuculline broadened the time frame for the detection of synaptic input, ZD7288 equalized the probability for a spike independent of the delay of the inputs, thereby abolishing coincidence detection within the delays tested.

Methodological Considerations

In vivo recordings from layer II/III and layer V pyramidal cells in anesthetized rats show spontaneous as well as whisker-deflection-correlated synaptic activity with low frequency and high amplitude (Helmchen *et al.*, 1999; Svoboda *et al.*, 1999; Zhu and Connors, 1999). This pattern reflects a highly synchronous input, which can result, at least in layer V pyramidal cells, in the generation of complex sodium–calcium spikes (Helmchen *et al.*, 1999). A comparable behavior with low EPSP and spiking frequencies was also found in layer II/III and V pyramidal cells of awake rats during whisking periods (Margrie *et al.*, 2002). In order to imitate these *in vivo* patterns, we used high-amplitude PSPs, which brought the cell from rest close to threshold.

Direct intracellular current injection was used in the majority of studies dealing with integrative processes in layer V dendrites (Berger *et al.*, 2001; Larkum *et al.*, 2001, Williams and Stuart, 2002), but not all (Pouille and Scanziani, 2001). This has the advantage that the exact localization of the induced potential changes is known. However, injection of currents instead of using conductance changes has the disadvantage that currents are not limited by their reversal potential and that shunting is neglected. For the study of the effects of shunting and leak conductances such as $GABA_A$ receptors and I_h we decided therefore to use extracellular stimulation in order to induce conductance changes. The response of each cell was calibrated in a such way that a threshold regime was reached where 50% of the trials resulted in a spike. If this maximal spiking probability was similar under control conditions and after application of a blocker, the width of the MSP–delay plot reflected the time window for coincidence detection. The inputs to layer V pyramidal cells were activated with stimulation electrodes positioned at the border between layers I and II. Under these conditions, stimulation could have led to the distal activation of layer V pyramidal cells via the excitatory fibers in layer I. However, activation of layer II/III pyramidal cells or of distally located GABAergic interneurons could indirectly activate more proximally situated synapses. In spite of the heterogeneity of the activated synaptic inputs, we found a relatively homogeneous effect of $GABA_A$ receptor activation and I_h on the coincidence detection window. This suggests that the detailed localization and composition of the synaptic inputs are of minor importance for the results reported in this study.

$GABA_A$ Receptors and Synaptic Integration in Layer V Pyramidal Cells

In this study, GABAergic input could completely prevent axonal action potential generation. This could be the result of a direct activation of the somatic GABAergic synapses (White, 1989) shunting the axonal sodium spike initiation and curtailing the synaptic event (Pouille and Scanziani, 2001). Under these conditions, distal PSPs could, however, evoke a dendritic spike (Williams and Stuart, 2002). In about half of our experiments with distal inputs, we found such a forward-propagating dendritic spike, while in the other half a back-propagating sodium spike was seen (Larkum *et al.*, 2001). Blocking the $GABA_A$ receptors changed this pattern only in a subset of cells. In these cells, extracellular stimulation resulted in the generation of somatic, back-propagating spikes. However, burst firing was seen in nearly all cells under block of the $GABA_A$ receptors. This correlates well with the observation that GABA receptors exert a veto effect on back-propagating action-potential-activated calcium spike firing (BAC-firing) in these cells (Larkum *et al.*, 1999). An alternative or additional mechanism would be a stronger excitatory drive with polysynaptic effects resulting in burst firing.

$GABA_A$ Receptors and Coincidence Detection in Layer V Pyramidal Cells

GABAergic input to layer V pyramidal cells is generated by a heterogeneous group of interneurons. Their axons terminate along the whole somatodendritic axis of the pyramidal cells (Somogyi *et al.*, 1998; Gupta *et al.*, 2000). However, there is a clear distribution of inhibitory and excitatory inputs: the overwhelming majority of the synapses on the soma and the dendritic shaft is GABAergic, while the majority of the excitatory synapses sits on spines (White, 1989; Keller, 1995). This distinguished position of the GABAergic input and the organization of interneurons as networks connected via both electrical and chemical synapses (Galarreta and Hestrin, 1999; Gibson *et al.*, 1999) can exert a strong influence on the summation properties and thus on coincidence detection. Bicuculline at 1 and 10 μM led to a broadening of the coincidence detection window for two incoming PSPs by factors of 1.9 and 3.4, respectively. This effect was also seen in hippocampal CA1 pyramidal cells (Pouille and Scanziani, 2001), while GABA application sharpened the time window for coincidence

detection in neurons of the chicken nucleus laminaris (Funabiki *et al.*, 1998). Iontophoretic application of bicuculline broadened and GABA sharpened the selectivity of the interaural time difference in the owl's midbrain (Fujita and Konishi, 1991), pointing to the importance of $GABA_A$ receptors for discrimination in the bird auditory system. The broadening of the coincidence detection window in layer V pyramidal cells was correlated with a prolongation of the decaying phase of the PSP – an effect which was not seen in all cells. This heterogeneity can be explained by a varying contribution of $GABA_A$ receptor activation to the PSP waveform. Activation of excitatory and inhibitory neurons can lead to an EPSP–IPSP sequence where the IPSP curtails the EPSP (Pouille and Scanziani, 2001). Alternatively, activation of $GABA_A$ receptors leads to a shunting of EPSPs by decreasing the cell's input resistance, resulting in a reduction of the membrane time constant and a consecutive acceleration of the EPSP decay time constant.

In contrast to what one would expect intuitively, in 58% of the cells studied the highest probability for eliciting an action potential was not found when both PSPs were activated simultaneously. If bicuculline or gabazine were applied to these 'asymmetric' cells, the coincidence plot became 'symmetric' to the origin in all cells tested. Such an asymmetric GABAergic activation and the consecutive shunting of one input by the other one could be well explained if one stimulation electrode activated a larger population of GABAergic cells than the other. In addition, unbalanced activation of GABAergic synapses along the somatodendritic axis of the cell could lead to asymmetric coincidence detection as well. Asymmetric activation of GABAergic networks could well serve as a physiological mechanism to control the time delay between two inputs leading to action potential generation. Such an asymmetric GABAergic activation was not seen in CA1 pyramidal cells after coincident Schaffer collateral activation (Pouille and Scanziani, 2001). These authors stimulated directly an excitatory input which was followed by di-synaptic feed-forward inhibition. In the present study, the extracellular stimulation activated directly both excitatory and inhibitory axons of unknown origins, resulting in a heterogeneous pattern of symmetric and asymmetric responses.

I_h and Coincidence Detection in Layer V Pyramidal Cells

Similar to $GABA_A$ receptor activation, I_h exerted its effects on coincidence detection via the active shortening of the decaying phase of the PSP (Nicoll *et al.*, 1993). In addition, blockade of I_h increased the input resistance of neocortical pyramidal cell dendrites (Berger *et al.*, 2001). However, due to their opposing spatial distributions along the somatodendritic axis, modulation of $GABA_A$ receptors and I_h should result in different shunting patterns. Due to the high density of I_h channels in the distal apical dendrite, the effect will be more pronounced for distal than for proximal inputs. The resulting reduction of temporal summation in pyramidal cells (Magee, 1998; Williams and Stuart, 2000, 2002; Berger *et al.*, 2001) makes the temporal influence of each EPSP more precise with regard to synaptic integration. In contrast to $GABA_A$ receptors, block of I_h always led to a prolongation of the PSP decaying phase. This is due to the fact that all layer V pyramidal cells contain I_h channels, while the proportion of active $GABA_A$ receptors was variable, depending on the stimulation situation.

Functional Implications

Layer V pyramidal cells handle the integration of signals from thousands of spatially distributed excitatory and inhibitory synapses. These cells can detect highly coincident excitatory inputs using voltage- and ligand-gated conductances such as I_h and $GABA_A$ receptors. In addition, these pyramidal cells respond with a qualitatively different spiking pattern if inputs to distal and proximal regions of the cell are activated within a narrow time window – BAC firing (Larkum *et al.*, 1999). A single spike is generated if the sodium spike initiation zone is activated alone. In contrast, simultaneous activation of both the axonal and dendritic spike initiation zones results in a burst discharge (Larkum *et al.*, 1999). The coincident activation of the different cell compartments leads therefore to a change of the output, reflecting the importance of this associative process. For an effective detection of coincident proximal and distal inputs, a narrow time window is essential. This can be achieved by synaptic events with a fast decay time course, which allow summation only during a short time period. Distal synaptic events are shortened by I_h channels located on the apical dendrite (Berger *et al.*, 2001), while proximal synaptic events are curtailed by somatically localized $GABA_A$ receptors. As a consequence, abolishing these PSP-curtailing mechanisms would lead to a strong broadening of the time window for BAC firing and therefore to a loss of the precision of this process. Because BAC firing provides a potential mechanism for binding the information from different brain areas (Singer and Gray, 1995), precise coincidence detection seems to be an essential mechanism during the integration of sensory information in layer V pyramidal cells. In addition, the observed time shifts in coincidence detection due to unbalanced activation of inhibitory input could provide the basis for encoding temporal and spatial sensory information (Ahissar and Arieli, 2001).

Notes

We thank Mrs K. de Peyer and Cornelia Spengler for excellent technical assistance and Drs A. Rauch, W. Senn and D. Ulrich for helpful discussions and careful reading of earlier versions of this manuscript. Supported by the Swiss National Science Foundation (grant SNF 3100-061335.00), the Silva Casa Stiftung (H.-R.L.), the Théodore-Ott Foundation and the Bonizzi–Theler Foundation (T.B.).

Address correspondence to Dr Thomas Berger, Institute of Physiology, University of Bern, Bühlplatz 5, CH-3012 Bern, Switzerland. Email: berger@pyl.unibe.ch.

References

Ahissar E, Arieli A (2001) Figuring space by time. Neuron 32:185–201.

Berger T, Larkum ME, Lüscher H-R (2001) High I_h channel density in the distal apical dendrite of layer V pyramidal cells increases bidirectional attenuation of EPSPs. J Neurophysiol 85:855–868.

Cauller LJ, Connors BW (1994) Synaptic physiology of horizontal afferents to layer I in slices of rat SI neocortex. J Neurosci 14:751–762.

deCharms RC, Zador A (2000) Neural representation and the cortical code. Annu Rev Neurosci 23:613–647.

Farinas I, DeFelipe J (1991) Patterns of synaptic input on corticocortical and corticothalamic cells in the cat visual cortex. I. The cell body. J Comp Neurol 304:53–69.

Fujita I, Konishi M (1991) The role of GABAergic inhibition in processing of interaural time difference in the owl's auditory system. J Neurosci 11:722–739.

Funabiki K, Koyano K, Ohmori H (1998) The role of GABAergic inputs for coincidence detection in the neurones of nucleus laminaris of the chick. J Physiol (Lond) 508:851–869.

Galarreta M, Hestrin S (1999) A network of fast-spiking cells in the neocortex connected by electrical synapses. Nature 402:72–75.

Gibson JR, Beierlein M, Connors BW (1999) Two networks of electrically coupled inhibitory neurons in neocortex. Nature 402:75–79.

Gray CM (1999) The temporal correlation hypothesis of visual feature integration: still alive and well. Neuron 24:31–47.

Gupta A, Wang Y, Markram H (2000) Organizing principles for a diversity of GABAergic interneurons and synapses in the neocortex. Science 287:273–278.

Harris NC, Constanti A (1995) Mechanism of block by ZD 7288 of the hyperpolarization-activated inward rectifying current in guinea pig substantia nigra neurons *in vitro*. J Neurophysiol 74:2366–2378.

Helmchen F, Svoboda K, Denk W, Tank DW (1999) *In vivo* dendritic calcium dynamics in deep-layer cortical pyramidal neurons. Nat Neurosci 2:989–996.

Ito Y, Koshiba T, Doi M, Asami S, Fukuda H, Murakoshi Y (1992) Characterization of antagonistic activity and binding properties of SR 95531, a pyridazinyl-GABA derivate, in rat brain and cultured cerebellar neuronal cells. Synapse 10:326–333.

Keller A (1995) Synaptic organization of the barrel cortex. In: Cerebral cortex, vol. 11: the barrel cortex of rodents (Jones EG, Diamond IT, eds), pp. 221–262. New York: Plenum.

Kisley MA, Gerstein GL (1999) The continuum of operating modes for a passive model neuron. Neural Comput 11:1139–1154.

König P, Engel AK, Roelfsema PR, Singer W (1996) Coincidence detection or temporal integration. The role of the cortical neuron revisited. Trends Neurosci 19:130–137.

Larkum ME, Zhu JJ (2002) Signaling of layer 1 and whisker-evoked Ca^{2+} and Na^{+} action potentials in distal and terminal dendrites of rat neocortical pyramidal neurons *in vitro* and *in vivo*. J Neurosci 22:6991–7005.

Larkum ME, Zhu JJ, Sakmann B (1999) A new cellular mechanism for coupling inputs arriving at different cortical layers. Nature 398: 338–341.

Larkum ME, Zhu JJ, Sakmann B (2001) Dendritic mechanisms underlying the coupling of the dendritic with the axonal action potential initiation zone of adult rat layer 5 pyramidal neurons. J Physiol (Lond) 533:447–466.

Magee JC (1998) Dendritic hyperpolarization-activated currents modify the integrative properties of hippocampal CA1 pyramidal neurons. J Neurosci 18:7613–7624.

Magee JC (1999) Voltage-gated ion channels in dendrites. In: Dendrites (Stuart G, Spruston N, Häusser M, eds), pp.139–160. New York: Oxford University Press.

Margrie TW, Brecht M, Sakmann B (2002) *In vivo*, low-resistance, whole-cell recordings from neurons in the anaesthetized and awake mammalian brain. Pflügers Arch Eur J Physiol 444:491–498.

Migliore M, Shepherd GM (2002) Emerging rules for the distribution of active dendritic conductances. Nat Neurosci 3:362–370.

Nicoll A, Larkman A, Blakemore C (1993) Modulation of EPSP shape and efficacy by intrinsic membrane conductances in rat neocortical pyramidal neurons *in vitro*. J Physiol (Lond) 468:693–710.

Pape H-C (1996) Queer current and pacemaker: the hyperpolarization-activated cation current in neurons. Annu Rev Physiol 58:299–327.

Pouille F, Scanziani M (2001) Enforcement of temporal fidelity in pyramidal cells by somatic feed-forward inhibition. Science 293: 1159–1163.

Santoro B, Grant SGN, Bartsch D, Kandel ER (1997) Interactive cloning with the SH3 domain of N-src identifies a new brain specific ion channel protein, with homology to Eag and cyclic nucleotide channels. Proc Natl Acad Sci USA 94:14815–14820.

Schiller J, Schiller Y, Stuart G, Sakmann B (1997) Calcium action potentials restricted to distal apical dendrites of rat neocortical pyramidal neurons. J Physiol (Lond) 505:605–616.

Shadlen MN, Movshon JA (1999) Synchrony unbound: a critical evaluation of the temporal binding hypothesis. Neuron 24:67–77.

Singer W, Gray CM (1995) Visual feature integration and the temporal correlation hypothesis. Annu Rev Neurosci 18:555–586.

Somogyi P, Gábor T, Lujan R, Buhl EH (1998) Salient features of synaptic organisation in the cerebral cortex. Brain Res Rev 26:113–135.

Svoboda K, Helmchen F, Denk W, Tank DW (1999) Spread of dendritic excitation in layer 2/3 pyramidal neurons in rat barrel cortex *in vivo*. Nat Neurosci 2:65–73.

White EL (1989) General organization of the cerebral cortex. In: Cortical circuits: synaptic organization of the cerebral cortex (White EL, ed.), pp. 19–45. Boston, MA: Birkhäuser.

Williams SR, Stuart GJ (2000) Site independence of EPSP time course is mediated by dendritic I_h in neocortical pyramidal neurons. J Neurophysiol 83:3177–3182.

Williams SR, Stuart GJ (2002) Dependence of EPSP efficacy on synapse location in neocortical pyramidal neurons. Science 295:1907–1910.

Yuste R, Gutnick MJ, Saar D, Delaney KR, Tank DW (1994) Ca^{2+} accumulations in dendrites of neocortical pyramidal neurons: an apical band and evidence for two functional compartments. Neuron 13:23–43.

Zhu JJ (2000) Maturation of layer 5 neocortical pyramidal neurons: amplifying salient layer 1 and layer 4 inputs by Ca^{2+} action potentials in adult rat tuft dendrites. J Physiol (Lond) 526:571–587.

Zhu JJ, Connors BW (1999) Intrinsic firing patterns and whisker-evoked synaptic responses of neurons in rat barrel cortex. J Neurophysiol 81:1171–1183.